THE JOURNAL OF
PHYSICAL CHEMISTRY B

ARTICLE

pubs.acs.org/JPCB

Second- and Third-Order Nonlinearities of Novel Push−Pull Azobenzene Polymers

Hasnaa El Ouazzani,[†] Konstantinos Iliopoulos,[†] Mindaugas Pranaitis,[†] Oksana Krupka,[‡] Vitaliy Smokal,[‡] Aleksey Kolendo,[‡] and Bouchta Sahraoui[†,*]

[†]Institut des Sciences et Technologies Moléculaires d'Angers, MOLTECH ANJOU, CNRS UMR 6200, Université d'Angers, 2 Bd Lavoisier, 49045 Angers cedex

[‡]Kyiv Taras Shevchenko National University, 60 Volodymyrska, 01033 Kyiv Ukraine

ABSTRACT: In this work, the second- and third-order nonlinear optical response of spin-deposited thin films of three different push−pull side chain azobenzene polymers is investigated by the second- and third-harmonic Maker fringes techniques using 30 ps laser pulses at a fundamental wavelength of 1064 nm. Measurements were carried out before and after aligning the chromophores by corona poling of the films, while different polarization configurations have been utilized. Strong dependence of the response upon the structure of the systems has been found, which is related to the different charge transfer within the molecules. The reported findings are compared with already published results.

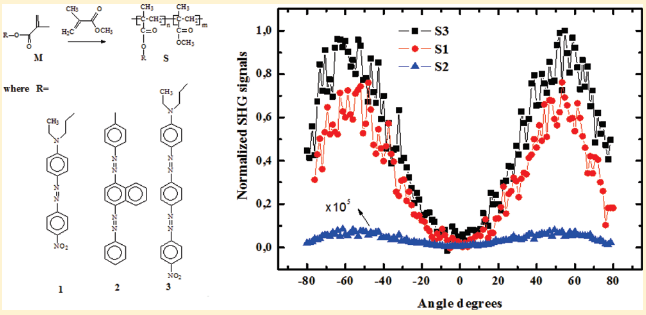

1. INTRODUCTION

Recently polymer/azobenzene nonlinear optical (NLO) systems are widely investigated, as they can be of great importance for a variety of applications. The azobenzene moieties can be either doped into the polymer matrixes or covalently attached to the polymer.[1−4] The latter case usually results in more stable systems with increased density of chromophores and enhanced nonlinear optical response.[5] The strong nonlinearity emanates from the strong charge transfer taking place within these units.[6] Among the azobenzenes, the Disperse Red 1 is one of the most widely investigated, and many studies can be found in the literature.[7−19]

Intensive research has been carried out in previous years to investigate the second-order nonlinear optical response of azobenzene/polymer systems (e.g., refs 7−9, 20, 21). The additional attribute of these systems of photoinduced trans−cis and vice versa isomerization renders them promising candidates for applications like optical data storage, surface relief gratings, photoswitching, alignment of liquid crystals, optical elements, and so forth.[10,11,22−26] An important prerequisite to achieve high second harmonic generation (SHG) is to make the systems noncentrosymmetric by aligning the chromophores. This can be done in several ways including electrode poling, corona poling, all optical poling, and so forth.[1] The corona poling is widely used, and it is based on applying a dc electric field while heating the film near the glass-transition temperature (T_g) to increase the mobility of the chromophores.[7] Then, by still applying the electric field, the system is cooled to room temperature. In this way, when the electric field is switched off, the orientations of the dipole moments remain frozen for a long time depending upon the chemical structure and the T_g of the systems.

Apart from the SHG, more recently, the third harmonic generation (THG) efficiency of azobenzenes has been also studied.[14−19,27−32] The third-order nonlinear susceptibility ($\chi^{(3)}$) contains terms which are resonant at ω, 2ω, and 3ω, and so it is expected to be more easily altered by changes regarding the conformation of the molecule. In this sense, the knowledge of the $\chi^{(3)}$ can be utilized for the visualization of modifications concerning the molecular structure.[29] The advantage of the THG technique is that it can provide information only about the electronic contribution to the $\chi^{(3)}$ without being influenced from generally slower contributions like molecular orientation. Azo dyes exhibit usually high $\chi^{(3)}$ values which are very important for applications like optical switching and optical limiting. However, the knowledge of the connection between several parameters like π-delocalization, donor−acceptor groups, orientation, and the $\chi^{(3)}$, which is needed for tailoring the nonlinear response to match the needs of specific applications, is not fully acquired yet.

In this direction, it is very important to characterize both the second- and the third-order nonlinearity. In this work, we investigate a series of push−pull side chain azobenzene polymers (Figure 1) by the well-known SHG, THG Maker fringes setup[33−35] using the same laser excitation source. In particular, comparative study is carried out between the novel S2, S3 systems (Figures 1, 2) and one of the most studied quasi 1D charge transfer molecules with enhanced first hyperpolarizability, which is the DR1 grafted to the copolymer S (i.e. S1 system). Apart from the investigation of the third-order and the second-order nonlinear optical response of the systems, the impact of the electron-acceptor group and the

Received: October 16, 2010
Revised: December 22, 2010
Published: February 16, 2011

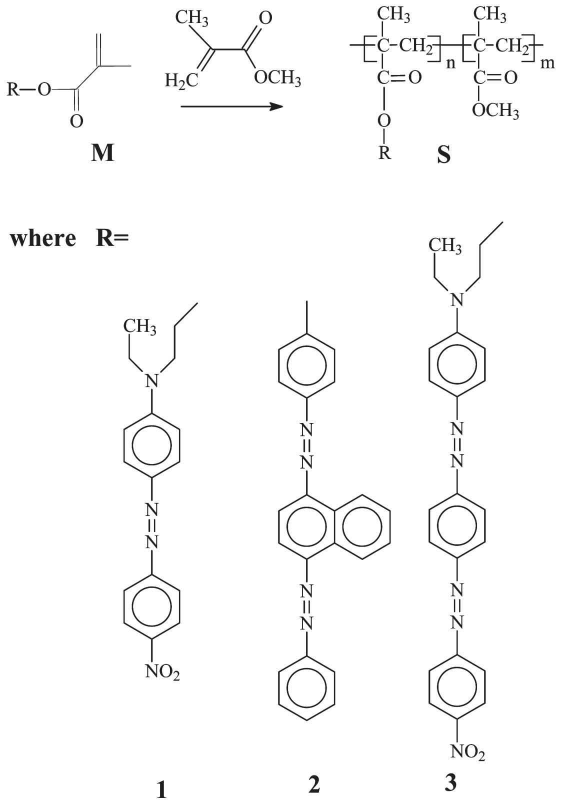

Figure 1. Investigated azopolymers.

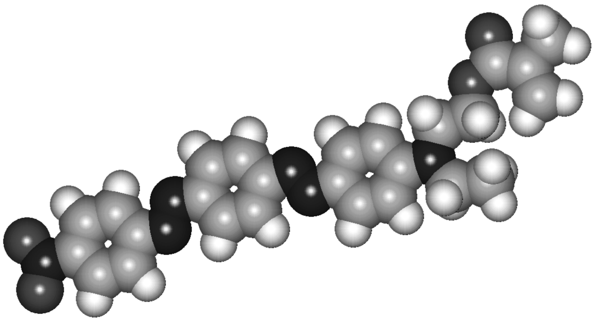

Figure 2. Molecule model of monomer M3.

charge transfer within the azobenzene moieties of the systems as well as of the alignment of the chromophores with the corona poling on the nonlinearity is presented and discussed.

2. EXPERIMENTAL SECTION

2.1. Nonlinear Optical Techniques. The second/third-order nonlinear optical response was studied by the SHG/THG Maker fringes setup in transmission employing the fundamental exit (1064 nm) of a 30 ps mode-locked Nd:YAG laser with 1 Hz repetition rate. The beam had Gaussian temporal and spatial profile, and by passing through a $\lambda/2$ wave plate and a polarizer, the intensity and the polarization were precisely adjusted. A low-power reflection was measured with a photodiode in order to allow recording of the incident laser intensity throughout the measurements. Then, the laser beam was focused by a 250 mm lens on the sample, which had been positioned near the focal plane, on a rotational stage allowing the variation of the incident angle with a resolution of 0.5° around the normal of the incident beam. A second polarizer positioned after the sample offered the possibility to change the detection polarization direction between s and p thus allowing investigation of different polarization configurations. After passing through a KG3 filter, which cut out the fundamental beam, as well as an interference filter (at 532 nm for SHG or at 355 for THG) to preserve only the SHG/THG signal, the latter was detected with a photomultiplier (PMT), which was connected with a boxcar and computer in order to be averaged and recorded. Neutral density (ND) filters have been always positioned before the PMT to avoid saturation.

Concerning the SHG intensity, and in the case of an isotropic nonlinear material, neglecting reflections, the following expression stands:[33−35]

$$I_{2\omega}^{s-p}(\theta) = \frac{128\pi^5}{c\lambda^2}\frac{[t_{af}^{1s}]^4[t_{fs}^{2p}]^2[t_{sa}^{2p}]^2}{n_{2\omega}^2\cos^2\theta_{2\omega}} I_\omega^2(L\chi_{eff}^{(2)})^2 \times \exp[-2(\delta_1+\delta_2)]\frac{\sin^2\Phi+\sinh^2\Psi}{\Phi^2+\Psi^2} \qquad (1)$$

where I_ω is the intensity of the pump wave; λ is its wavelength; $\chi_{eff}^{(2)}$ is the effective second order nonlinear susceptibility; n_ω and $n_{2\omega}$ are the refractive indices of the pump and harmonic waves; L is the film thickness; and t_{af}^{1s}, t_{fs}^{2p}, and t_{sa}^{2p} are the Fresnel transmission coefficients (air−film−substrate−air system) for the fundamental and SHG beams. The phase angles Φ and Ψ are given by the following equations:[33]

$$\Phi = \frac{2\pi L}{\lambda}(n_\omega\cos\theta_\omega - n_{2\omega}\cos\theta_{2\omega})$$

$$\Psi = \delta_1 - \delta_2 = \frac{2\pi L}{\lambda}\left(\frac{n_\omega\kappa_\omega}{\cos\theta_\omega} - \frac{n_{2\omega}\kappa_{2\omega}}{\cos\theta_{2\omega}}\right) \qquad (2)$$

where θ_ω, $\theta_{2\omega}$ are the angles between the fundamental and doubled frequency beams and κ_ω, $\kappa_{2\omega}$ are the extinction coefficients of the nonlinear material at frequencies ω and 2ω. A 0.5 mm thick Y-cut quartz slab has been used as reference material for these measurements with $\chi^{(2)} = 8.07 \times 10^{-12}$ esu (1 pm/V) and coherence length 20.5 μm.

The alignment of the chromophores, which was necessary to break the centrosymmetrical attribute of the chromophores and to enhance the SHG response, has been done with the corona poling technique. During this procedure, the samples were heated to near the glass-transition temperature, and then a high voltage was applied through two 30 μm diameter tungsten wires, which had been placed 1 cm over the films, inducing a strong electric field. Then, the films were cooled down to room temperature, while the voltage was still applied.

For the analysis of the THG measurements and because the third harmonic signal is in a spectral position, where the linear absorption of the samples is important, the following equation has been used:[35,36]

$$\chi^{(3)} = \frac{2}{\pi}\chi_s^{(3)} l_c^S \frac{\alpha/2}{1-\exp(-\alpha l/2)}\sqrt{\frac{I_{3\omega}}{I_{3\omega}^S}} \qquad (3)$$

where $\chi^{(3)}$, $\chi_s^{(3)}$ are the third-order nonlinear susceptibilities of the sample and the reference material (silica in this case), respectively, l_c^S is the coherence length of fused silica, l is the film thickness, α is the linear absorption coefficient, and $I_{3\omega}$ and $I_{3\omega}^S$ are the peak intensities of the Maker fringes pattern of the film and the fused silica slab, respectively. The utilized reference $\chi^{(3)}$ value at 1064 nm for fused silica was $\chi_s^{(3)} = 2.0 \times 10^{-22}$ m^2 V^{-2}.[37]

Equation 3 allows the determination of the third-order nonlinear optical response in the case of films under the prerequisite that the thickness of the film is much lower than the coherence length and also that the signal coming from the substrate can be considered to be negligible compared to the signal emanating from the film. The latter has been verified in our work by in situ removing a part of the film and measuring the signal from the substrate. During the measurements, the films were positioned with the thin film side facing the detector.

2.2. Instrumentation. ^{1}H NMR (500 MHz) spectra were recorded by a Bruker Advance DRX-500 spectrometer. Chemical shifts are in ppm from the internal standard tetramethylsilane. UV−vis measurements were performed at room temperature either in solutions in a quartz liquid cell or as thin films deposited on glass substrates with a Perkin-Elmer UV/vis/NIR Lambda 19 spectrometer. A Q20 differential scanning calorimetry (DSC) model (TA Instruments) with a continuous N_2 purge was used to determine the glass and phase-transition temperatures (T_g) of all polymers. Two scans were run at a heating rate of 10 °C/min up to 200 °C followed by a cooling to 20 °C giving the values of T_g.

2.3. Synthesis and Thin Film Preparation. Standard distillation procedures were performed for triethylamine and tetrahydrofuran (THF) just prior to use. 2,2′-Azobis(isobutyronitrile) (AIBN) was recrystallized twice from absolute methanol. Methacrylic chloride was vacuum distilled immediately before use. Methylmethacrylate (MMA) was washed with aq NaOH to remove inhibitors and was dried with $CaCl_2$ under nitrogen at reduced pressure. The chromophores 4-(4-nitrophenylazo)aniline, *N*-ethyl-*N*-(2-hydroxyethyl)-4-(4-nitrophenylazo)aniline DR1, and 4-[4-(phenylazo)-1-naphthylazo]phenol DO13 were purchased from Aldrich and were purified by double recrystallization from an absolute methanol solution. All other reagents and solvents were commercially available and were used as received.

4-(N-Ethyl-N-(2-hydroxyethyl)amino)-4′-(4-nitrophenylazo)-azobenzene. 4-(4-Nitrophenylazo)aniline (5 g, 20.6 mmol) was dissolved in a solution of concentrated hydrochloric acid 10 mL and dimethylformamide (DMF) 80 mL. The reaction mixture was cooled down in an ice−water bath to 0 °C and was stirred for 15 min, and then a solution of sodium nitrite (1.45 g, 21 mmol) in 5 mL of water was added dropwise. The reaction mixture was stirred for 2 h at 0 °C, and then the *N*-ethyl-*N*-(2-hydroxyethyl)aniline (3.5 g, 21 mmol) in 15 mL of acetic acid was added dropwise. After stirring at 0−5 °C for 5 and 12 h at room temperature, a large amount of a dark precipitate formed. The precipitate was collected by filtration and then was washed with saturated sodium bicarbonate solution and was dried. The crude product was purified by column chromatography on silica gel (toluene:acetone, 1:1.5) followed by recrystallization from THF: hexane obtained as dark purple crystals mp 225 °C, 62%.

^{1}H NMR (500 MHz, DMSO-d6): δ 8.46(d, 2H, Ar−**H**), 8.00 (d, 2H, Ar−**H**), 8.12 (d, 4H, Ar−**H**), 7.85 (d, 2H, Ar−**H**), 6.90 (d, 2H, Ar−**H**), 4.85 (t, 1H, **OH**), 3.55−3.65 (m, 6H, $-CH_2-$), 1.18 (s, 3H, $-CH_3$). UV−vis (THF): λ = 346, 520 nm.

*4-((2-Methacryloyloxyethyl)ethylamino)-4-nitroazobenzene (**M1**).* Azomonomer was synthesized in the same way as reported.[38] The solid was recrystallized from methanol. Dark red crystals mp 83 °C, yield 80%. ^{1}H NMR (500 MHz, $CDCl_3$): δ 8.35 (d, 2H, Ar−**H**), 7.92 (t, 4H, Ar−**H**), 6.85 (d, 2H, Ar−**H**), 6.1 (s, 1H, CH_2), 5.6 (s, 1H, CH_2), 4.38 (m, 2H, OCH_2), 3.75 (m, 2H, NCH_2), 3.56 (m, 2H, NCH_2), 1.94 (s, 3H, CH_3), 1.24 (m, 3H, CH_3). UV−vis (THF): λ = 475 nm.

*4-[4-(Phenylazo)-1-naphthylazo]phenol (**M2**).* A solution of 4-[4-(phenylazo)-1-naphthylazo]phenol (1.5 g, 4.2 mmol) and triethylamine (0.64 g, 6.3 mmol) was dissolved in THF (40 mL). The solution was kept in an ice bath for 10 min. A solution of distilled methacryloyl chloride (0.66 g, 6.3 mmol) in THF (10 mL) was added slowly to the reaction mixture. After the addition of methacryloyl chloride, the solution was stirred for 12 h at ambient temperature. The solvent was removed by rotary evaporation, and the residue was washed with a solution of sodium carbonate (0.8 g) in water (40 mL). After removing the solvent, the resulting material was purified by column chromatography (silica gel, ethyl acetate/hexane 1/8). Red solid residue yield 75%, mp 90 °C.

^{1}H NMR (500 MHz, DMSO-d6): δ 9.01−8.98 (m, 2H, naphthalene), 8.14 (d, 2H, Ar−**H**), 8.05 (d, 2H, Ar−**H**), 7.92 (s, 2H, naphthalene), 7.85 (d, 2H, Ar−**H**), 7.78−7.81 (m, 2H, naphthalene), 7.63−7.58 (m, 3H, Ar−**H**), 6.35 (s, 1H, CH_2), 5.9 (s, 1H, CH_2), 2.07 (s, 3H, CH_3). UV−vis (THF): λ = 325, 428 nm.

*4-((2-Methacryloyloxyethyl)ethylamino)-4′-(4-nitrophenylazo)-azobenzene (**M3**).* Azomonomer **M3** was synthesized in the same way as azomonomer **M2**. Dark purple crystals yield 60%, mp 160 °C.

^{1}H NMR (500 MHz, $CDCl_3$): δ 8.40 (d, 2H, Ar−**H**), 8.12−7.92 (m, 8H, Ar−**H**), 6.85 (d, 2H, Ar−**H**), 6.12 (s, 1H, CH_2), 5.61 (s, 1H, CH_2), 4.38 (t, 2H, OCH_2), 3.75 (t, 2H, NCH_2), 3.55 (q, 2H, NCH_2CH_3), 1.97 (s, 3H, CH_3), 1.28 (s, 3H, CH_3). UV−vis (THF): λ = 340, 502 nm.

Polymerization. Polymers were synthesized by free-radical polymerization. The polymerization was carried out in 10 wt % toluene solution of **M1** and methylmethacrylate (MMA) with monomer initial mole ratios 1:3. The polymerization was conducted using AIBN as a free-radical initiator (1 wt % of monomer) at 80 °C 35 h in argon atmosphere. Previously, the initial mixture was degassed with repeated freeze−pump−thaw cycles. The polymerization was stopped by pouring the reaction mixture into methanol. This procedure was repeated several times to ensure removal of unreacted methacrylic monomers, and finally, the polymer S1 was dried under vacuum at 50 °C overnight. In the cases of copolymerization **M2** with MMA and **M3** with MMA, the same synthetic procedure was used in DMF and 1,4-dioxane solution accordingly. The copolymerization ratios in the corresponding polymers were calculated on the basis of the integrated peak areas of ^{1}H NMR spectra in DMSO-d_6 for S1 and S3 and in pyridine-d_5 for S2. The glass-transition temperatures were measured by differential scanning calorimetry to be 125, 110, and 140 °C for the copolymers S1, S2, and S3, respectively.

Thin Film Processing. Thin films of S1, S2, and S3 were obtained by spin coating of filtered solutions through a 0.4 μm pore size nylon syringe filter on BK7 glass slides. The principle of deposition (of the mixture with certain viscosity) is based on a homogeneous spreading out of the solution on the rotating substrate with an angular speed of 800 rpm. We used as solvent 1,1,2-trichlororethane for the quality of thin film formation. The same polymer concentration of 56 g/L was used. Immediately after the deposition, the films were cured in an oven at 50 °C and for 180 min in order to eliminate any remaining solvent. Their thickness was measured by a profilometer (Tencor, ALFA-Step) and in all cases was found to be 0.4−0.5 μm.

3. RESULTS AND DISCUSSION

The nonlinear optical response of thin films of the azobenzene polymers S1−S3 has been investigated by means of SHG/THG Maker fringes measurements. In Figure 3, characteristic absorption spectra of the investigated systems can be seen. As shown in the

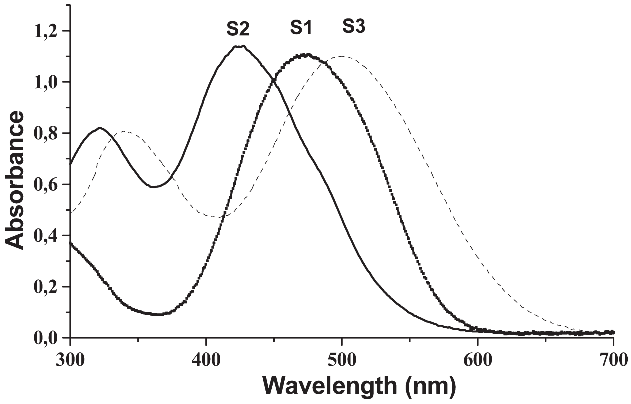

Figure 3. UV−vis spectra of S1, S2, and S3 in thin solid films.

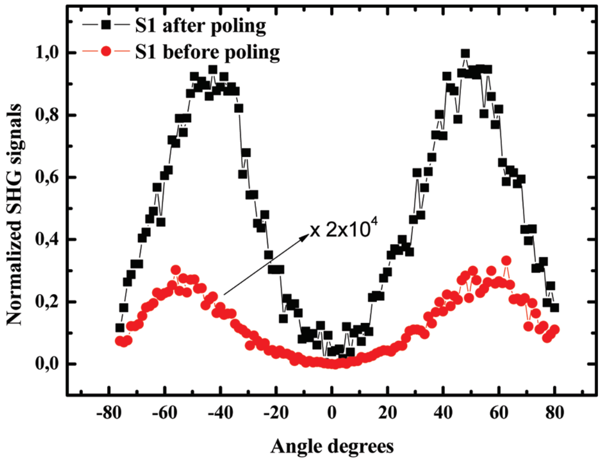

Figure 4. Normalized SHG Maker fringes patterns obtained for the S1 sample under p−p polarization configuration before and after corona poling.

figure, the $\pi-\pi^*$ band of the S1 and S3 systems is shifted to the red compared to the S2. This is due to the electron-donor and electron-acceptor substituents in the synthesized azobenzene polymers S1 and S3, which increase the charge-transfer character of the $\pi-\pi^*$ transition.[39] The fact that the S3 system exhibits maximum absorption at the longest wavelength (500 nm) among the investigated compounds reflects the highest charge-transfer interaction occurring between the electron-donor group (amino) and the electron-acceptor group (nitro). This enhancement of the charge-transfer efficiency, if compared to the S1 system, can be attributed to the additional phenyldiazene fragment in the side chain.[32]

Table 1. Effective $\chi^{(2)}$ Values Obtained for the S1, S2, and S3 Systems in the p−p Configuration before and after Corona Poling with Strong Electric Field

sample	$\chi^{(2)}$ (pm/V) before corona poling	$\chi^{(2)}$ (pm/V) after corona poling
S1	0.10	26
S2	n/a	0.56
S3	0.08	30

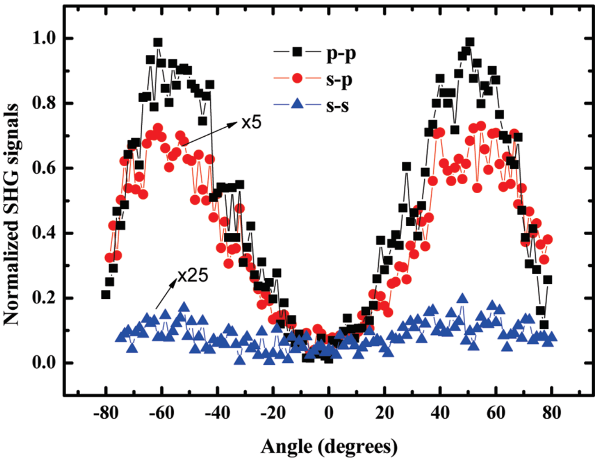

Figure 5. Comparative SHG Maker fringes patterns under the same experimental conditions, obtained for the S3 system, under three different polarization configurations.

First, SHG measurements were done before and after corona poling of the films for all studied push−pull azobenzene polymers S1−S3. In the case of the measurements after the corona poling, the experiments were carried out directly after the poling of the chromophores to avoid possible misalignment. However, a very slow disorientation with time after poling has been found, and the signal of the systems was significant and remained unchanged even a long time after the corona poling. The observed long-term stability is mainly attributed to the relatively high T_g of the studied systems (see Experimental Section). To illustrate the impact of the corona poling of the chromophores to the SHG response, the Maker fringes patterns obtained for the S1 system using p excitation and detection polarizations can be seen in Figure 4 before and after alignment of the chromophores. To enable visual clarity of the figure, the curve obtained before the corona poling has been multiplied by a factor of 2×10^4. Because of the huge difference of the response between the two measurements, different ND filters have been used to attenuate the signals, which have been in any case taken into account during the analysis of the experimental data. There is significant difference of the obtained SHG magnitude between the results before and after the corona poling as expected, which is attributed to very efficient alignment of the molecules by the applied electric field. Similar behavior has been found for the other two systems S2 and S3. This result can be clearly seen in Table 1 where the values corresponding to the p−p configuration can be seen for all the systems before and after the corona poling of the films. The increase in the nonlinearity for the S1 and S3 system after the corona poling is about a factor of 260 and 375 for the systems S1 and S3, while in the case of the system S2, the signal prior to corona poling has been too low to offer sufficient signal-to-noise ratio for these measurements. In all cases, strong nonlinearity has been found after the corona poling for all systems.

Then, comparative Maker fringes measurements were done between the S1, S2 and S3 azobenzene polymers using different excitation−detection polarization configurations ss, sp and pp. For all three investigated systems, the pp configuration has resulted in the strongest nonlinear optical response. Intermediate efficiency has been obtained for the s−p configuration, while the s−s corresponded to the lowest SHG efficiency. Especially in the case of the S2 system, where the electron-donating part is missing from the side chain, the s−s configuration resulted in very low signal-to-noise ratio which was not adequate for measurements. The comparison between the different configurations is nicely

Table 2. Effective $\chi^{(2)}$ Values for All Investigated Systems under s−s, s−p, and p−p Excitation−Detection Polarization Configurations

sample	$\chi^{(2)}$ (pm/V)		
	s−s	s−p	p−p
S1	3.26	10.79	26
S2	n/a	0.08	0.56
S3	2.16	9	30

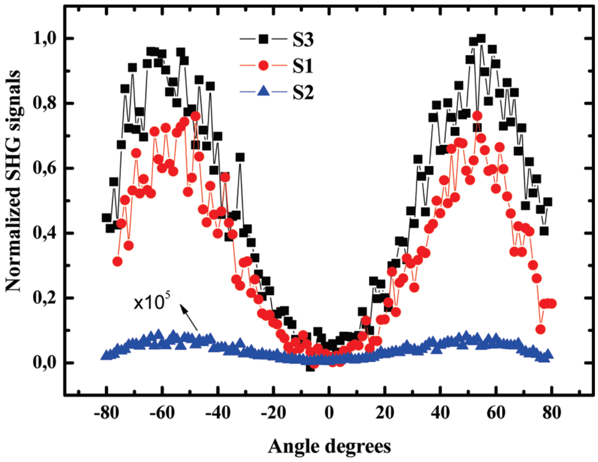

Figure 6. Normalized SHG Maker fringes curves enabling the comparison between the systems S1, S2, and S3 under identical experimental conditions.

illustrated in Figure 5, where the obtained curves are seen for the system S3, under identical experimental conditions for all three different configurations, after corona poling of the films. The curves corresponding to the sp and ss configurations are multiplied by a factor of 5 and 25, respectively. The big difference in the signal levels is obvious, while the maximum SHG signals correspond to an angle of about 55° and the minimum to normal incidence of the laser beam.

From Maker fringes patterns obtained for all the azobenzene polymers and for the ss, pp, and sp configurations, the effective values of $\chi^{(2)}$ have been determined using quartz as reference sample following the details provided in the Experimental Section and are shown in Table 2. Characteristic curves obtained for these systems are presented in Figure 6 for the pp polarization configuration. The $\chi^{(2)}$ values of the S1 and S3 systems are similar between these two systems but are much higher than that of the system S2. In particular for the pp configuration, the difference is about a factor of 50. This large enhancement can be attributed to the strong acceptor moieties in the para position and electron-donor group (amino) and results in the highest charge transfer in the polymer system, which has consequently a strong impact on the NLO response. The obtained results are in good agreement with already reported results in the literature. In ref 40, pDR1M azobenzene homopolymer films were studied, and comparative investigation was carried out between the pp and ss configurations, which revealed higher signal with the former configuration in agreement with the present findings (see Figure 5). The value found here for the reference S1 system is in agreement with already published values in the literature.[9,40,41]

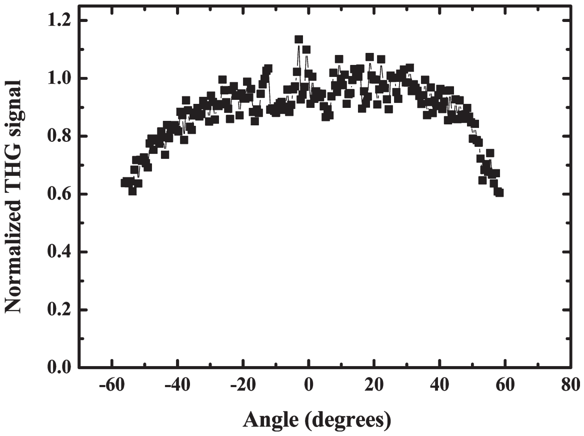

Figure 7. Characteristic THG curve corresponding to the S3 sample (pp polarization configuration).

Table 3. Third-Order Nonlinear Susceptibility ($\chi^{(3)}$) under All Polarization Configurations

sample	$\chi^{(3)}$ (10^{-22} m^2/V^2)			
	polarization configurations			
	p−p	s−s	s−p	p−s
S1	2432	2420	1584	1574
S2	147	148	118	112
S3	618	612	416	432

Then, THG measurements were carried out in fresh, noncorona-poled films of the same compounds using different polarization configurations. It was found that the ss and pp polarization configurations led to higher signals, while the difference between them was within the experimental error. On the contrary, when different excitation and detection polarizations (ps or sp configurations) were used, the signal was reduced to significantly lower values. As an example, the obtained THG signal as a function of the incident angle can be seen in Figure 7 corresponding to the S3 sample and p polarization for both excitation and detection. The $\chi^{(3)}$ values for the polarization configurations pp, ss, sp, and ps of the samples S1, S2, and S3, obtained before the orientation of the chromophores, according to the procedure described in the Experimental Section, are presented in Table 3. In all cases, the values were found to be very high, indicative of very efficient third harmonic generation of the azobenzenes, which were up to 3 orders of magnitude higher than the values obtained for the reference material. The value reported by Yoon et al.[42] for poly(1,4-phenylenevinylene) containing Disperse Red is about 7 times lower than that reported here, which can be attributed to the different structures of the systems as well as to the fact that the measurements reported there were carried out at 1907 nm, in transparent region for the system. Moreover, the $\chi^{(3)}$ values of the S2 and S3 systems found here are several times lower if compared with the S1 system. More specifically, in the case of the pp configuration, the efficiency of the S2 and S3 systems is decreased by about 16 and 4 times, respectively, with respect to the S1 system. In agreement with the SHG results, the nonlinearity of the S1 and S3 is much higher than that of S2 because of the enhanced charge transfer of these systems. A comparative second series of experiments have been done for all possible polarization configurations after corona poling of the samples, but the results have been found in all cases to be identical, which

Table 4. Third-Order Nonlinear Susceptibility ($\chi^{(3)}$) for the Systems S1−S3 before and after Corona Poling

sample	$\chi^{(3)}$ (10^{-22} m^2/V^2)	
	before corona poling	after corona poling
S1	2432	2442
S2	147	144
S3	618	612

could be expected as the third harmonic generation is not expected to have significant dependence upon the alignment of the molecules.[43] In Table 4, the third-order nonlinear susceptibilities before and after the corona poling can be seen for the pp case and for all the investigated systems. The differences were found to be within the experimental error of the measurements. We show that the novel azobenzene polymers exhibit very high second and third order nonlinearity, which can be tailored by proper chemical functionalization, including appropriate electron−donor acceptor groups. This fact is due to the modification of the charge transfer within the molecule, as well as to the strong impact of the latter on the NLO response.[44,45]

4. CONCLUSIONS

We designed and synthesized NLO polymers with different sizes of the conjugated system between donor and acceptors. Both the second harmonic and the third harmonic generations of the systems have been studied by the Maker fringes techniques. The second- and third-order nonlinear optical parameters have been found to be very high in all cases. The big differences between the nonlinearity of the systems are discussed. The significant nonlinear optical response combined with the possibility to further modify it, by changing the conjugation, the electron-acceptor and the electron-donor groups, suggests that these systems can prove to be important candidates for a variety of photonic/opto-electronic applications.

■ AUTHOR INFORMATION

Corresponding Author

*E-mail: bouchta.sahraoui@univ-angers.fr.

■ ACKNOWLEDGMENT

The authors would like to thank the COST action MP0702 (Towards Functional Sub-Wavelength Photonic Structures) for financial support. They would like to thank also C. Cassagne, A. Mahot, and D. Guichaoua for their technical help.

■ REFERENCES

(1) Burland, D. M.; Miller, R. D.; Walsh, C. A. *Chem. Rev.* **1994**, *94*, 31.
(2) Hampsch, H. L.; Yang, J.; Wong, G. K.; Torkelson, J. M. *Macromolecules* **1988**, *21*, 526.
(3) Loucif-Saibi, R.; Nakatani, K.; Delaire, J. A.; Dumont, M.; Sekkat, Z. *Chem. Mater.* **1993**, *5*, 229.
(4) Eich, M.; Sen, A.; Looser, H.; Bjorklund, G. C.; Swaien, J. D.; Twieg, R.; Yoon, D. Y. *J. Appl. Phys.* **1989**, *66*, 2559.
(5) Yesodha, S. K.; Sadashiva Pillai, C. K.; Tsutsumi, N. *Prog. Polym. Sci.* **2004**, *29*, 45.
(6) Kulakowska, J.; Kucharski, S. *Eur. Polym. J.* **2000**, *36*, 1805.
(7) Nahata, A.; Shan, J.; Yardley, J. T.; Wu, C. *J. Opt. Soc. Am. B* **1993**, *10*, 1553.
(8) Singer, K. D.; Kuzyk, M. G.; Sohn, J. E. *J. Opt. Soc. Am. B* **1987**, *4*, 968.
(9) Singer, K. D.; Sohn, J. E.; Lalama, S. J. *Appl. Phys. Lett.* **1986**, *49*, 248.
(10) Gindre, D.; Boeglin, A.; Fort, A.; Mager, L.; Dorkenoo, K. D. *Opt. Express* **2006**, *14*, 9896.
(11) Czaplicki, R.; Krupka, O.; Essaidi, Z.; El.-Ghayoury, A.; Kajzar, F.; Grote, J. G.; Sahraoui, B. *Opt. Express* **2007**, *15*, 15268.
(12) Yoon, C. B.; Lee, J. I.; Shim, H. K. *Synth. Met.* **1997**, *84*, 273.
(13) Meredith, G.; Vandusen, J. G.; Williams, D. J. *Macromolecules* **1982**, *15*, 1385.
(14) Brzozowski, L.; Sargent, E. H. *J. Mater. Sci.: Mater. Electron.* **2001**, *12*, 483.
(15) Rangel-Rojo, R.; Yamada, S.; Matsuda, H.; Yankelevich, D. *Appl. Phys. Lett.* **1998**, *72*, 1021.
(16) Churikov, V. M.; Hsu, C.-C. *J. Opt. Soc. Am. B* **2001**, *18*, 1722.
(17) Matsumoto, S.; Kubodera, K. I.; Kurihara, T.; Kaino, T. *Appl. Phys. Lett.* **1987**, *51*, 1.
(18) Muto, S.; Kubo, T.; Kurokawa, Y.; Suzuki, K. *Thin Solid Films* **1998**, *322*, 233.
(19) Kuzyk, M. G.; Sohn, J. E.; Dirk, C. W. *J. Opt. Soc. Am. B* **1990**, *7*, 842.
(20) Ortyl, E.; Chan, S. W.; Nunzi, J.-M.; Kucharski, S. *Opt. Mater.* **2006**, *29*, 268.
(21) Si, J.; Qiu, J.; Kitaoka, K.; Hirao, K. *J. Appl. Phys.* **2001**, *89*, 2029.
(22) Eaton, D. *Science* **1991**, *253*, 281.
(23) Kawata, S.; Kawata, Y. *Chem. Rev.* **2000**, *100*, 1777.
(24) Hagen, R.; Bieringer, T. *Adv. Mater.* **2001**, *13*, 1805.
(25) Natansohn, A.; Rochon, P. *Adv. Mater.* **1999**, *11*, 1387.
(26) Sekkat, Z.; Knoll, W. *Photoreactive Organic Thin Films*; Academic Press: New York, 2002.
(27) He, T.; Cheng, Y.; Du, Y.; Mo, Y. *Opt. Commun.* **2007**, *275*, 240.
(28) Gherab, K. N.; Gatri, R.; Hank, Z.; Dick, B.; Kutta, R.-J.; Winter, R.; Luc, J.; Sahraoui, B.; Fillaut, J.-L. *J. Mater. Chem.* **2010**, *20*, 2858.
(29) Churikov, V. M.; Hsu, C. C. *Appl. Phys. Lett.* **2000**, *77*, 2095.
(30) Lee, H.-J.; Won, Y.-H.; Kang, S.-J.; Choi, S.-K.; Kim, H. K. *J. Polym. Sci., Part A: Polym. Chem.* **1996**, *34*, 2333.
(31) Dong, F.; Koudoumas, E.; Couris, S.; Shen, Y.; Qiu, L.; Fu, X. *J. Appl. Phys.* **1997**, *81*, 7073.
(32) Qian, Y.; Xiao, G.; Wang, G.; Lin, B.; Cui, Y.; Sun, Y. *Dyes Pigm.* **2007**, *75*, 218.
(33) Herman, W. N.; Hayden, L. M. *J. Opt. Soc. Am. B* **1995**, *12*, 416.
(34) Jerphagnon, J.; Kurtz, S. K. *J. Appl. Phys.* **1970**, *41*, 1667.
(35) Sahraoui, B.; Luc, J.; Meghea, A.; Czaplicki, R.; Fillaut, J.-L.; Migalska-Zalas, A. *J. Opt. A: Pure Appl. Opt.* **2009**, *11*, 1.
(36) Kanbara, H.; Maruno, T.; Yamashita, A.; Matsumoto, S.; Hayashi, T.; Konami, H.; Tanaka, N. *J. Appl. Phys.* **1996**, *80*, 3674.
(37) Gubler, U.; Bosshard, C. *Phys. Rev. B* **2000**, *61*, 10702.
(38) Ho, M. S.; Natansohn, A.; Rochon, P. *Macromolecules* **1995**, *28*, 6124.
(39) Li, N.; Lu, J.; Xia, X.; Xu, Q.; Wang, L. *Polymer* **2009**, *50*, 428.
(40) Rodriguez, V.; Adamietz, F.; Sanguinet, L.; Buffeteau, T.; Sourisseau, C. *J. Phys. Chem. B* **2003**, *107*, 9736.
(41) Mortazavi, M. A.; Knoesen, A.; Kowel, S. T.; Higgins, B. G.; Dienes, A. *J. Opt. Soc. Am. B* **1989**, *6*, 733.
(42) Yoon, C. B.; Lee, J. I.; Shim, H. K. *Synth. Met.* **1997**, *84*, 273.
(43) Schnabel, W. *Polymers and Light: Fundamentals and Technical Applications*; Wiley-VCH Verlag GmbH & Co: Weinheim, 2007; p 396.
(44) Derkowska, B.; Mulatier, J. C.; Fuks, I.; Sahraoui, B.; Nguyen Phu, X.; Andraud, C. *J. Opt. Soc. Am. B* **2001**, *18*, 610.
(45) Terkia-Derdra, N.; Andreu, R.; Sallé, M.; Levillain, E.; Orduna, J.; Garin, J.; Orti, E.; Viruela, R.; Pou-AméRigo, R.; Sahraoui, B.; Gorgues, A.; Favard, J.-F.; Riou, A. *Chem.—Eur. J.* **2000**, *6*, 1199.